The Use of Serological Assays to Monitor Spatial and Temporal Spread of Citrus Tristeza Virus in Symptomless Trees in Eastern Spain

T. R. Gottwald, M. Cambra, and P. Moreno

ABSTRACT. Citrus tristeza virus (CTV) was monitored by monoclonal and polyclonal antibody probes via ELISA in six symptomless orange and grapefruit orchards in the Valencian Community, Spain for up to 12 yr. Linear, exponential, monomolecular, logistic, Gompertz, and Weibull temporal models were fitted to each of the data sets by linear and nonlinear regression analysis. Overall the nonlinear Gompertz model was the most appropriate based on correlation of observed vs. predicted values and examination of residuals of regression for patterns. The Gompertz rate parameter k was 0.205 to 0.413 for orange and 0.078 for grapefruit in areas of high CTV incidence, and 0.077 to 0.093 for orange orchards in areas with lower CTV incidence. Ordinary runs analysis indicated little within- or across-row association of CTV-positive trees, indicating that disease in trees immediately adjacent to one another was not highly associated. Morisita's index (MI) of dispersion for different quadrat sizes was inconclusive for most plots. Significant MI values occurred only for plots with low (<0.1) disease incidence values, thus indicating only infrequent aggregation of CTV-positive trees. Spatial proximity patterns resulting from spatial autocorrelation analysis indicated associations among CTV-positive trees 8 to 24 trees apart but little or no association among adjacent trees and gave some insight into possible underlying processes of CTV spread. This lack of association among adjacent trees is consistent with ordinary runs and MI values. The stronger association among CTV-positive trees located at some distance from one another compared to immediately adjacent trees suggests possible patterns of viruliferous vector movement. Perhaps when aphid vectors take flight they preferentially move to trees farther away rather than to immediately adjacent trees.

Citrus tristeza virus (CTV) was first recognized as a problem in eastern Spain in 1957 following a severe freeze in 1956. Epidemics of CTV first appeared in the Ribera Alta district, Valencia, and were especially severe on sweet orange and mandarins grown on sour orange rootstock (8, 21). Since that time CTV has spread throughout much of Spain, most likely the result of movement of infected budwood and propagating materials. In the Valencian Community to date, an estimated 15 million CTV-infected trees on sour orange have died and many more are presently in decline. Since 1968 citrus nurseries in Spain have been forbidden to propagate sweet orange, mandarin, and grapefruit on sour orange and this policy has resulted in a systematic replacement of trees that had died, or were in severe decline with others on Carrizo or Troyer citrange, or other tolerant rootstocks (7, 8, 22).

The incidence and distribution of CTV in the Valencia area have increased considerably since they were first mapped and the continued spread of the disease is of concern to Valencian growers (7, 8). CTV incidence and movement have been related to the presence of *Aphis gossypii* Glover, *Aphis spiraecola* Patch and *Toxoptera aurantii* (Fons.) (16). *A. gossypii* is the most efficient vector in Spain and its populations have greatly increased in recent years (17). The development of monoclonal antibodies and the use of ELISA for detection and differentiation of mild and severe strains of CTV have opened a new era for CTV epidemiology research (6, 25, 28, 29). Such assays have made rapid detection and confirmation of large numbers of samples feasible and can be used to monitor CTV spread over time (10, 22). Because of the long perennial duration of most tree crop epidemics, only a few have been modeled over time. Temporal and spatial analyses have been conducted for a few citrus diseases such as citrus canker

Mention of a trademark, warranty, proprietary product, or vendor does not constitute a guarantee by the U.S. Department of Agriculture and does not imply its approval to the exclusion of other products or vendors that may also be suitable.

and greening (12, 13, 15). For citrus tristeza, modeling and simulations have previously been attempted but only from limited data (10,22).

The purpose of this study was to examine the spatial and temporal dynamics of CTV in tolerant scion-rootstock combinations in the Valencia region in an attempt to develop models for prediction of rates of disease increase and spatial patterns of spread, and by detailed analysis to better understand spatial dissemination of CTV over time.

MATERIALS AND METHODS

Data were collected over a 12-yr period from six plantings in the Valencian Community. All plantings were on Troyer citrange or Cleopatra mandarin rootstocks and therefore symptomless for CTV. All of the plots were established from indexed CTV-negative mother plants and were disease-free when planted and all were assayed annually. Two of the test plots, IVIA 3&4 and IVIA 6&7, consisted of 216 trees each of Washington navel orange on Troyer citrange planted in 1978 on a 2-m × 6-m spacing. Both plots were located on the grounds of the Instituto Valenciano de Investigaciones Agrarias, near Moncada, Valencia, Spain, and were assayed yearly from 1984 to 1992. The El Realengo plot consisted of 400 Marsh Seedless grapefruit on Troyer citrange planted on a 5.5-m × 5.5-m spacing located on the El Realengo citrus farm in the Ribera Alta district in southern Valencia established in 1973. In 1982, indexed CTV-free trees of Redblush grapefruit on Troyer citrange were interplanted among the rows. These trees were removed in 1991. The El Realengo plot was assayed yearly from 1981 to 1991. The Los Valles plot consisted of 408 Navelina orange on Cleopatra mandarin trees planted on a 6.5-m × 4.0-m spacing located near Sagunto, Valencia, established in 1973 and was assayed yearly from 1981 to 1991. The Orihuela plot consisted of 495 trees of Newhall navel orange on Troyer citrange interplanted in 1979 among the rows of an older navel-on-sour orange planting located in Orihuela, Alicante. This former planting was established in a 6-m × 4-m spacing and the interplanted trees on Troyer citrange followed the same pattern. About five percent of the trees were CTV-infected at replanting time. Most of the CTV-infected trees had been topworked to lemon as soon as tristeza symptoms began to appear. This plot was bordered by lemon plantings on two sides, vegetable crops on one side, and a planting of sweet orange on sour orange on the fourth side and was assayed yearly from 1984 to 1991.

Traditional aphid control procedures were used in all plots. These consisted of spraying two to six times per year mostly in the spring, depending on aphid population numbers, with dimethoate, methyl-oxidemethon, imiadoprin, carbemma oxyprimide, or cipermethrin.

Sample collection and analysis. All trees in each plot were sampled yearly in May or September. Three young apical shoots, 10 cm long, were collected from different parts of each tree and analyzed by the procedure previously described (8). Conventional ELISA-DAS methods with polyclonal antibodies from different antisera sources were used in 1981 and 1982 (11). From 1983 to 1989 ELISA-DAS was performed with monoclonal antibody 3DF1 (28). From 1989 to present the analysis was done by the ELISA-DAS biotin/streptavidin system using a commercially available mixture of monoclonal antibodies 3DF1 and 3CA5 (Ingenasa Co., Madrid, Spain) (4, 5, 28).

Temporal analysis. The disease incidence (number of infected trees divided by the total number of trees) of each plot was calculated for each year of the study. The appropriateness of the linearized and nonlinear forms of the linear, exponential, monomolecular, logistic, and Gompertz models was examined by linear regression analysis of transformed disease incidence data (2, 18, 27). Preliminary results from the linear regression analysis allowed the selection of parameters for the nonlinear regression analysis. Nonlinear regression analysis of nontransformed data from each plot was performed for the nonlinear forms (derivatives) of the

same models, (SAS NONLIN procedure, SAS Institute, Inc., Cary, North Carolina, USA: version 6.02). In addition, the Weibull nonlinear model was fitted to the data sets. The appropriateness of each model was determined by examining the coefficient of regression, the correlation coefficient of observed vs. detransformed predicted values, and the plots of residuals of regression vs. predicted values. Models of the highest coefficient of correlation were chosen as superior, as long as no patterns were seen in the residual plots (18).

Spatial analysis. Several methods of spatial analysis were used to attempt to determine how CTV spreads in citrus groves. Aggregation of diseased plants within and across rows of trees was determined by ordinary runs analysis (ORA) (20). Aggregation was assessed as the proportion of within- and across-row segments with significant ($P = 0.05$) clustering.

Aggregation was examined also by variance-to-mean ratio, Lloyd's index of patchiness, Lloyd's index of mean crowding, and Morisita's index of dispersion (23, 26). Prior to testing the data for aggregation by these techniques, the data from each plot were quadratized to parcel the data into counts of diseased trees. Each plot for each year was quadratized into 2×2, 4×4, and if possible 8×8 tree blocks. The sum of the diseased trees was calculated for each quadrat and the resulting data sets were used to calculate the various indices. Although all of the indices were calculated, because of the flexibility of Morisita's index and its compatibility with spatial autocorrelation analyses, it was chosen as the most appropriate and the only one which will be presented here. For Morisita's index (MI), disease is considered regularly distributed if $MI<1$, random if $MI=1$, and aggregated if $MI>1$ (23).

A final technique, spatial lag autocorrelation analysis (SLA), was employed to determine if noncontiguous spatial patterns exist which would not be indicated by MI or other indices of dispersion (9, 20, 24). The technique requires quadratized data, and in this case 2×2 quadratized data was used. Spatial lag autocorrelation analysis of the 2×2 quadrats for each year was accomplished with the LCOR2 program (14).

RESULTS

Analysis of temporal disease progress. The disease progress curves are depicted in Fig. 1A-E. The disease in-

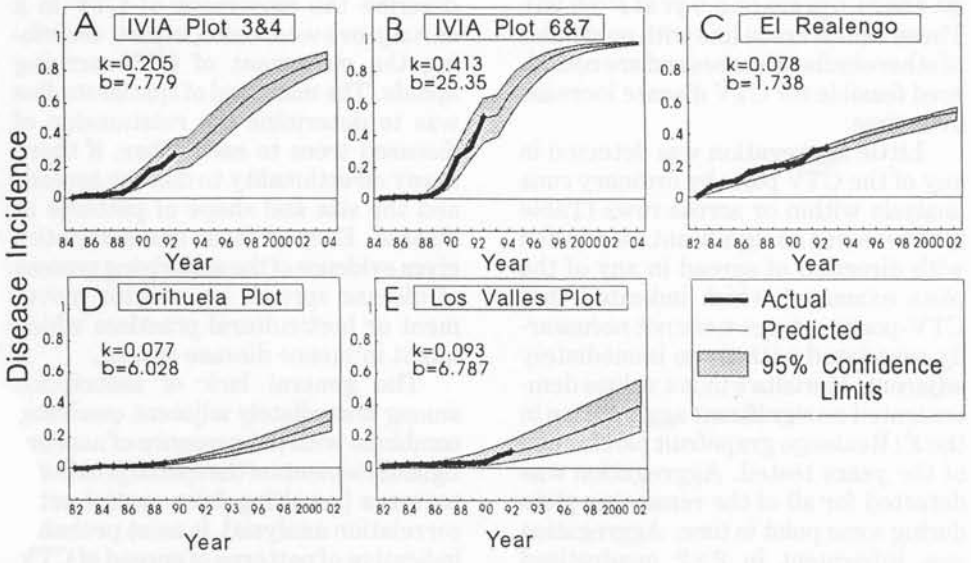

Fig. 1. Gompertz nonlinear model predictions of citrus tristeza virus increase in five citrus plots in eastern Spain. k = Gompertz rate parameter.

cidence in all of the plots, with the exception of El Realengo, was either in or entering the exponential phase of increase, as is common during the first half of an epidemic. Disease progress of CTV in the El Realengo plot was more linear than for the other plots and had not entered a logarithmic increase phase to date. The Weibull model was not applicable to any of the data sets and was discarded after several attempts. The best model was the nonlinear Gompertz (Table 1 and 2). The good fit of the Gompertz models is due to the present phase of the epidemics. The flexibility of this model and its ability to predict feasible future disease incidence values are its strengths. The Gompertz rate parameter k varied from 0.077 to 0.413 for the various orange plots and was 0.078 for the El Realengo grapefruit plot. Predictions of future disease incidence values were calculated by employing the various versions of the nonlinear Gompertz model (Fig. 1). Based on the above models for orange groves, if we assume a beginning disease incidence of 1%, in areas of high CTV incidence such as near Moncada, Valencia, CTV is predicted to achieve 50% disease incidence in 4.5 to 9.2 years (± 1.5 yr at $P = 0.05$), whereas in areas with low disease incidence 50% disease incidence is predicted to occur after 20.4 to 24.6 years (± 3.0 yr at $P = 0.05$). These values are in line with epidemics of other similar diseases and are considered feasible for CTV disease increase over time.

Little aggregation was detected in any of the CTV plots by ordinary runs analysis within or across rows (Table 3). There was no significant association with direction of spread in any of the plots examined which indicated that CTV-positive trees were not necessarily associated with those immediately adjacent. Morisita's index values demonstrated no significant aggregation in the El Realengo grapefruit plot for any of the years tested. Aggregation was detected for all of the remaining plots during some point in time. Aggregation was infrequent in 2×2 quadratized data early in the epidemics, then became slightly more prevalent in 4×4 and 8×8 quadratized data sets later in the epidemics (Fig. 2 A, B). This was expected because as disease increases, the size of individual patches of disease also increases. The associations were weak, for the most part, and inconclusive by MI analysis.

Results of spatial lag autocorrelation analysis for the CTV data from each plot have been condensed to graphs of the predicted proximity patterns for easier interpretation (Fig. 3). Noncontiguous proximity patterns frequently occurred in all of the CTV plots during some of the years. Only few quadrats next to the origin were significant, whereas patterns 4, 5, 7, and 12 lags (8 to 24 trees) away were seen. The presence of these discontinuous elements of the proximity patterns and general lack of association between adjacent quadrats indicated relationships among CTV-positive trees located at some distance from one another rather than immediately adjacent.

DISCUSSION AND CONCLUSIONS

The main complication for the CTV pathosystem is the movement of the virus by aphid vectors, particularly *A. gossypii* (16). Thus, in attempting to describe the movement of CTV in a citrus grove we are also, in part, describing the movement of CTV-carrying aphids. The main goal of spatial studies was to determine the relationship of diseased trees to each other, if there is any directionality to disease spread, and the size and shape of patterns of disease. Each of these characteristics gives evidence of the underlying process of disease spread, i.e., vector movement or horticultural practices which might influence disease spread.

The general lack of association among immediately adjacent quadrats, combined with the presence of noncontiguous elements of the spatial proximity patterns [resulting from spatial autocorrelation analysis], is most probably indicative of patterns of spread of CTV resulting from aphid vector dissemina-

TABLE 1
LINEAR REGRESSION ANALYSIS OF THE INCIDENCE OF CITRUS TRISTEZA VIRUS IN GROVES IN THE VALENCIAN COMMUNITY, SPAIN OVER TIME DETECTED BY ELISA

Model[z]	Plot	Coefficient of determination (r^2)	Slope (b)	Standard error of slope	Correlation (r) of observed vs. predicted values[y]	Range of disease incidence	Pattern present in residuals
Linear	IVIA Plot 3,4	0.846	0.033	0.005	0.920	0.014-0.278	+
Expo	IVIA Plot 3,4	0.964	0.396	0.029	0.988	0.014-0.278	+
Mono	IVIA Plot 3,4	0.829	0.038	0.007	0.904	0.014-0.278	+
Logit	IVIA Plot 3,4	0.960	0.434	0.033	0.990	0.014-0.278	+
Gompit	IVIA Plot 3,4	0.931	0.157	0.016	0.982	0.014-0.278	+
Linear	IVIA Plot 6,7	0.767	0.061	0.013	0.876	0.014-0.532	+
Expo	IVIA Plot 6,7	0.938	0.490	0.048	0.989	0.014-0.532	+
Mono	IVIA Plot 6,7	0.715	0.082	0.019	0.832	0.014-0.532	+
Logit	IVIA Plot 6,7	0.923	0.572	0.062	0.986	0.014-0.532	+
Gompit	IVIA Plot 6,7	0.862	0.237	0.036	0.963	0.014-0.532	+
Linear	El Realengo	0.963	0.028	0.002	0.981	0.173-0.485	−
Expo	El Realengo	0.926	0.089	0.008	0.971	0.173-0.485	−
Mono	El Realengo	0.958	0.043	0.003	0.981	0.173-0.485	−
Logit	El Realengo	0.948	0.132	0.010	0.977	0.173-0.485	−
Gompit	El Realengo	0.959	0.079	0.005	0.980	0.173-0.485	−
Linear	Los Valles	0.689	0.007	0.002	0.830	0.008-0.099	+
Expo	Los Valles	0.891	0.204	0.024	0.932	0.008-0.099	−
Mono	Los Valles	0.680	0.007	0.002	0.825	0.008-0.099	+
Logit	Los Valles	0.887	0.212	0.025	0.929	0.008-0.099	−
Gompit	Los Valles	0.844	0.059	0.008	0.906	0.008-0.099	−
Linear	Orihuela	0.933	0.005	0.001	0.966	0.004-0.039	−
Expo	Orihuela	0.836	0.376	0.068	0.979	0.004-0.039	−
Mono	Orihuela	0.932	0.005	0.001	0.965	0.004-0.039	−
Logit	Orihuela	0.839	0.381	0.068	0.980	0.004-0.039	−
Gompit	Orihuela	0.890	0.084	0.012	0.986	0.004-0.039	−

[z]Coefficients of determination (r^2) and slopes (b) were estimated by linear regression of transformed disease incidence over time. Disease incidence values were transformed by y, ln(y), ln(1/(1–y)), ln(y/1–y)), and –ln(–ln(y)) for linear, exponential, monomolecular, logistic, and Gompertz transformations, respectively.

[y]Correlation coefficients (r) of predicted values against observed values and the presence or absence of patterns in residual plots were examined for appropriateness of models.

TABLE 2
NONLINEAR REGRESSION ANALYSIS OF THE INCIDENCE OF CITRUS TRISTEZA VIRUS IN GROVES IN THE VALENCIAN COMMUNITY, SPAIN, OVER TIME DETECTED BY ELISA

Model[z]	Plot	Parameter	Estimate	Asymptotic standard error	Asymptotic 95% confidence limits		Correlation coef. (r) of observed vs. predicted values[y]	Pattern present in residuals
					Lower	Upper		
Linear	IVIA Plot 3,4	r	0.023	0.003	0.016	0.030	0.920	+
Expo	IVIA Plot 3,4	r	0.657	0.011	0.630	0.683	0.963	+
Mono	IVIA Plot 3,4	r	0.025	0.004	0.016	0.033	0.910	+
Logit	IVIA Plot 3,4	r	0.697	0.012	0.669	0.725	0.977	+
Gompit	IVIA Plot 3,4	k	0.205	0.017	0.165	0.244	0.991	−
		b	7.779	0.977	5.468	10.089		
Linear	IVIA Plot 6,7	r	0.037	0.007	0.021	0.053	0.876	+
Expo	IVIA Plot 6,7	r	0.725	0.008	0.707	0.744	0.978	+
Mono	IVIA Plot 6,7	r	0.042	0.010	0.019	0.064	0.854	+
Logit	IVIA Plot 6,7	r	0.804	0.008	0.784	0.823	0.991	−
Gompit	IVIA Plot 6,7	k	0.413	0.041	0.317	0.509	0.991	−
		b	25.352	7.846	6.798	43.906		
Linear	El Realengo	r	0.050	0.004	0.042	0.059	0.981	+
Expo	El Realengo	r	0.589	0.031	0.521	0.658	0.808	+
Mono	El Realengo	r	0.068	0.005	0.057	0.080	0.980	+
Logit	El Realengo	r	0.703	0.053	0.584	0.822	0.872	+
Gompit	El Realengo	k	0.078	0.006	0.066	0.091	0.980	−
		b	1.738	0.066	1.588	1.889		
Linear	Los Valles	r	0.006	0.001	0.004	0.007	0.830	−
Expo	Los Valles	r	0.419	0.007	0.404	0.435	0.979	−
Mono	Los Valles	r	0.006	0.001	0.004	0.008	0.826	+
Logit	Los Valles	r	0.428	0.008	0.411	0.445	0.976	−
Gompit	Los Valles	k	0.093	0.015	0.058	0.128	0.938	−
		b	6.787	0.988	4.552	9.022		
Linear	Orihuela	r	0.004	0.000	0.003	0.005	0.966	−
Expo	Orihuela	r	0.471	0.013	0.442	0.501	0.967	−
Mono	Orihuela	r	0.004	0.000	0.003	0.005	0.965	−
Logit	Orihuela	r	0.476	0.013	0.446	0.506	0.968	−
Gompit	Orihuela	k	0.077	0.006	0.062	0.093	0.987	−
		b	6.029	0.255	5.406	6.652		

[z]Model parameters were estimated by nonlinear regression of the integrated equations $y = rt$, $y = y_0e^{rt}$, $y = 1 - (1 - y_0)e^{rt}$, $y = 1/[1 + \exp^{-(\ln(y_0/1-y_0)) + rt}$, $y = \exp^{-Be-kt}$ for the linear, exponential, monomolecular, logistic, and Gompertz models, respectively, where r and k are rate parameters, y is disease incidence of trees, and t is time in years. For the Gompertz model, $B = -\ln(y_0)$.

[y]Coefficients of correlation (r) of predicted values against observed values and the presence or absence of patterns in residual plots were examined for appropriateness of models.

TABLE 3
ORDINARY RUNS ANALYSIS OF CITRUS TRISTEZA VIRUS IN SIX PLOTS IN EASTERN SPAIN

Plot	Direction	1981	1982	1983	1984	1985	1986	1987	1988	1989	1990	1991	June 1991
Plot 3&4	N-S	—	—	—	0/12[z]	0/12	0/12	0/12	0/12	0/12	3/12	3/12	1/12
	E-W	—	—	—	0/18	0/18	0/18	0/18	0/18	1/18	1/18	1/18	1/18
Plot 6&7	N-S	—	—	—	0/12	0/12	0/12	0/12	0/12	0/12	2/12	2/12	2/12
	E-W	—	—	—	0/18	0/18	0/18	0/18	0/18	0/18	0/18	0/18	1/18
El Realengo	N-S	1/20	1/20	1/20	1/20	0/20	0/20	0/20	0/20	0/20	1/20	1/20	—
	E-W	0/20	1/20	1/20	1/20	0/20	0/20	0/20	0/20	1/20	1/20	1/20	—
Parcela No. 3	N-S	—	—	—	—	—	—	—	1/24	—	3/24	—	—
	E-W	—	—	—	—	—	—	—	0/38	—	1/38	—	—
Los Valles	N-S	0/17	1/17	0/17	0/17	0/17	0/17	0/17	0/17	1/17	0/17	1/17	—
	E-W	0/24	0/24	0/24	0/24	0/24	2/24	2/24	2/24	1/24	0/24	0/24	—
Orihuela	N-S	—	—	—	1/15	1/15	1/15	1/15	2/15	2/15	2/15	2/15	—
	E-W	—	—	—	0/33	0/33	0/33	0/33	0/33	0/33	0/33	0/33	—

[z]Values shown are the number of test rows with significant aggregation ($P = 0.05$) divided by the total number of rows tested.

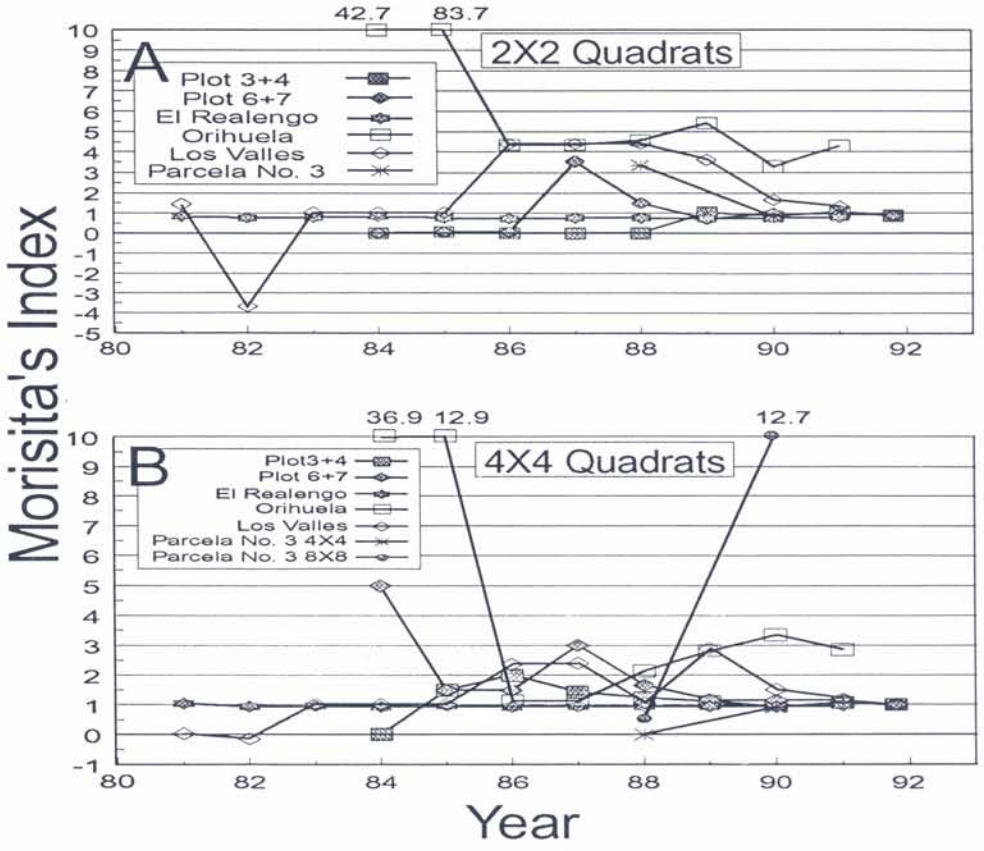

Fig. 2. Morisita's index of dispersion (MI) values for 2 × 2 and 4 × 4 quadrat sizes by year for citrus plots in eastern Spain infected with citrus tristeza virus. Because of the large size of Parcela No. 3, it was also possible to calculate a Morisita's index value for an 8 × 8 quadrat size. MI = 1 indicates a random distribution, MI < 1 indicates a regular distribution, and MI > 1 indicates aggregation of disease-containing quadrats.

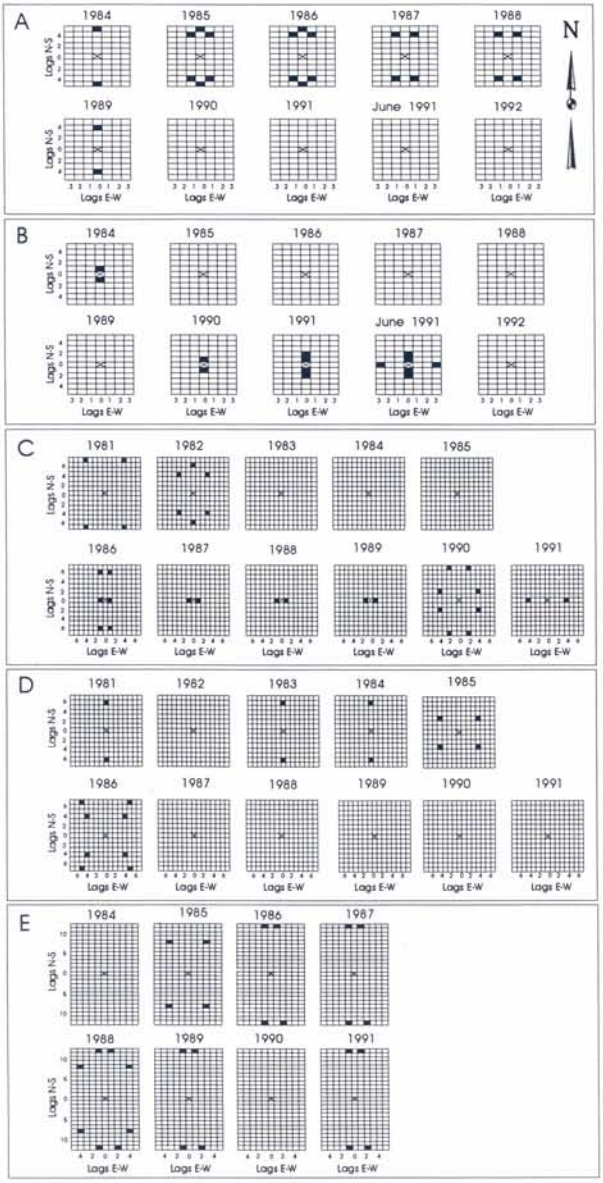

Fig. 3. Spatial proximity patterns of significant autocorrelations of citrus tristeza virus by year in citrus plots in eastern Spain infected with citrus tristeza virus. A) Plot 3&4, B) Plot 6&7, C) Los Valles, D) El Realengo, and E) Orihuela. Graphic representations of proximity patterns were derived from correlograms of spatial lag autocorrelations of 2 × 2 quadratized data for each plot during each year of the study. The 'X' in the middle of each pattern indicates the 0,0 lag position. Squares indicate spatial lags (quadrats) in relationship to the 0,0 lag position. The patterns are oriented with the vertical axis representing the north-south lags and the horizontal axis representing the east-west lags. Black rectangles denote significant positive autocorrelations ($P \leq 0.05$) at the indicated spatial lag positions. Note noncontiguous significant positive autocorrelations which most often occur at some distance to the center of the proximity patterns. For example in A) Plot 3&4 for 1984 positive autocorrelations occurred at lags 0,5 and 0,–5 along the north-south axis indicating that there was a relationship among quadrats of CTV-positive trees located 5 quadrats or 10 trees apart.

tion. This means that when CTV spreads, it does not spread to immediately adjacent trees but more often is associated with trees at some distance (i.e., 8, 10, 14, or 24 trees away [range 8-24 trees]). This finding provides insight into the underlying processes of disease spread. Aphid vectors (winged alates), which are the presumed means of CTV movement and infection, may preferentially move several trees away rather than to the immediately adjacent tree. This would explain the general lack or inconsistency of aggregation found in ordinary runs analysis and in indices of dispersion and the distance between significant noncontiguous lags in SLA.

Possible scenarios involved in aphid dissemination of CTV strains are best presented graphically (Fig. 4). In many insect-vectored diseases, viruliferous vectors move to immediately adjacent trees at random causing a 'clustered' disease distribution (Fig. 4A). Vector movement can also be 'directional' when vectors are disturbed in response to grove traffic or other environmental stimulus such as wind, etc., as in the case of psyllids carrying the greening pathogen (12), and result in elongated clusters of diseased trees (Fig. 4B). In the case of the CTV/aphid pathosystem in eastern Spain, apparently the aphid vectors do not move to the immediately adjacent tree but instead are attracted to trees farther away when they take flight. This would be represented by a more 'nondirectional' vector movement over longer distances and would give rise to CTV distribution patterns with trees being more related to those at some distance rather than to those immediately adjacent (Fig 4C). The growth characteristics of trees such as flush, color of foliage, etc., have been demonstrated to have an effect on aphid attraction. Perhaps tree growth habit, aphid population numbers, and numbers of alate aphids should also be included in future, more complex spatial and temporal models of CTV.

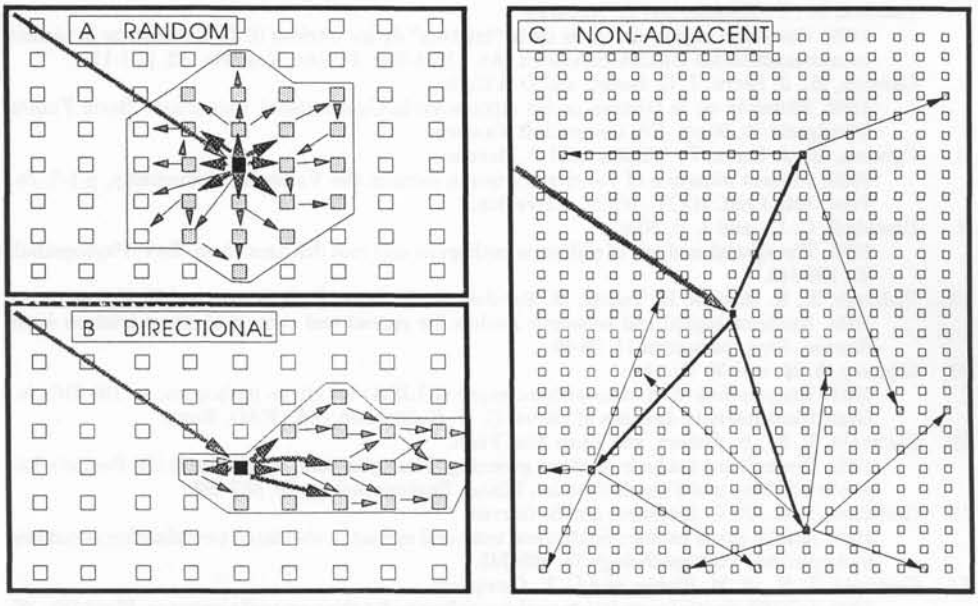

Fig. 4. Possible viruliferous vector movement scenarios. A) random nondirectional movement would give rise to a more or less circular aggregation of diseased trees. B) directional movement down rows in response to environmental stimulus would give rise to elongated clusters of diseased individuals. C) Nonadjacent movement of vectors which traverse some distance or number of trees before alighting would give rise to a seemingly random distribution which is actually aggregated but at some range of distance relative to the normal flight range of the vector. This distance can be detected by spatial autocorrelation analysis (refer to Fig. 3).

ACKNOWLEDGMENTS

We are thankful to E. Camarasa, T. Gorris, M. E. Martines, and J. Piquer of IVIA, Moncada, Valencia for technical assistance in collecting and/or processing samples. This work was funded by CAICYT (Project 727); Spain-USA Committee for Scientific and Technical Cooperation (Grant 156); IVIA (Projects 3053 and 8179) and Commission of the European Communities, Contract N. CT90-0783. The first author visited the IVIA to analyze the data presented herein, supported by a fellowship from the Conselleria de Cultura, Educacion y Ciencia de la Generalitat Valenciana.

LITERATURE CITED

1. Bar-Joseph, M., S. M. Garnsey, D. Gonsalves, M. Moscovitz, D. E. Purcifull, M. F. Clark, and G. Loebenstein.
1979. The use of enzyme-linked immunosorbent assay for detection of citrus tristeza virus. Phytopathology 69: 190-194.
2. Berger, R. D.
1981. Comparison of the Gompertz and logistic equations to describe plant disease progress. Phytopathology 71: 716-719.
3. Cambra, M., L. Batista, M. T. Yorris, S. M. Garnsey, and G. Carbonell.
1992. Use of double antibody sandwich indirect (DAS-I) ELISA with coating antibodies of different specificities for detection of citrus tristeza virus (CTV). Phytopathology 82: 607 (Abstr.).
4. Cambra, M., E. Camarasa, M. T. Gorris, S. M. Garnsey, and E. Carbonlee.
1991. Comparison of different immunosorbent assays for citrus tristeza virus (CTV) using CTV-specific monoclonal and polyclonal antibodies. p. 38-45. *In:* Proc. 11th Conf. IOCV. IOCV, Riverside.
5. Cambra, M., S. M. Garnsey, T. A. Permar, C. T. Henderson, D. Gumpf, and C. Vela.
1990. Detection of citrus tristeza virus (CTV) with a mixture of monoclonal antibodies. Phytopathology 80: 1034 (Abstr.).
6. Cambra, M., P. Moreno, and L. Navarro.
1979. Detección rápida del virus de la "tristeza" de los cítricos (CTV), mediante la técnica immunoenzimática ELISA-Sandwich. An. INIA/Ser. Protec. Veg. No. 12, p. 1-11.
7. Cambra, M., J. Serra, J. C. Bonet, and D. Villalba.
1990. Situación de la tristeza de los cítricos en la Communidad Valenciana. Serie Fullets Divulgació 30, 90 pp. Ed. Generalitat Valencia.
8. Cambra, M., J. Serra, D. Villalba, and P. Moreno.
1988. Present situation of the citrus tristeza virus in the Valencian Community, p 1-7. *In:* Proc. 10th Conf. IOCV. IOCV, Riverside.
9. Campbell, C. L., and J. P. Noe.
1985. The spatial analysis of soilborne pathogens and root diseases. Ann. Rev. Phytopathol. 23: 129-148.
10. Fishman, S., R. Marcus, H. Talpaz, M. Bar-Joseph, Y. Oren, R. Salomon, and M. Zohar.
1983. Epidemiological and economic models for spread and control of citrus tristeza virus disease. Phytoparasitica 11: 39-49.
11. Garnsey, S. M. and M. Cambra.
1991. Enzyme-linked immunosorbent assay (ELISA) for citrus pathogens, p. 193-216. *In:* Graft transmissable diseases of citrus. C. N. Roistacher, (ed.) FAO, Rome.
12. Gottwald, T. R., B. Aubert, and Zhao Xue-Yuan.
1989. Preliminary analysis of citrus greening (Huanglungbin) epidemics in the People's Republic of China and French Reunion Island. Phytopathology 79: 687-693.
13. Gottwald, T. R., R. G. McGuire, and S. Garran.
1988. Asiatic citrus canker: Spatial and temporal spread in simulated new planting situations in Argentina. Phytopathology 78: 739-745.
14. Gottwald, T. R., S. M. Richie, and C. L. Campbell.
1992. LCOR2-Spatial correlation analysis software for the personal computer. Plant Dis. 76: 213-215.
15. Gottwald, T. R., L. W. Timmer, and R. G. McGuire.
1991. Analysis of disease progress of citrus canker in nurseries in Argentina. Phytopathology 79: 1276-1283.
16. Hermoso de Mendoza, A., J. F. Ballester Olmos, and J. A. Pina Lorca.
1984. Transmission of citrus tristeza virus by aphids (Homoptera, Aphidinea) in Spain. p 23-27. *In:* Proc. 9th Conf. IOCV. IOCV, Riverside.

17. Hermoso de Mendoza, A., and P. Moreno.
1989. Cambios cuantitativos en la fauna afídica de los cítricos Valencianos. Bol. San. Veg. Plagas 15: 139-142.
18. Madden, L. V.
1986. Statistical analysis and comparison of disease progress curves, p. 55-84. *In:* Plant Disease Epidemiology: Population dynamics and management. K. Leonard and W. E. Fry, (eds.). Macmillan, New York.
19. Madden, L. V., R. Louie, J. J. Abt, and J. K. Knoke.
1982. Evaluation of tests for randomness of infected plants. Phytopathology 72: 195-198.
20. Modjeska, J. S. and J. O. Rawlings.
1983. Spatial correlation analysis of uniformity data. Biometrics 39: 373-384.
21. Moreno, P., L. Navarro, C. Fuertes, J. A. Pina, J. F. Ballester, A. Hermoso de Mendoza, J. Juarez, and M. Cambra.
1983. La tristeza de los agrios problemática en España. Hoja Técnica No. 47, IVIA, Madrid, España.
22. Moreno, P., J. Piquer, J. A. Pina, J. Juarez, and M. Cambra.
1988. Spread of citrus tristeza virus in a heavily infested citrus area in Spain, p. 71-76. *In:* Proc. 10th Conf. IOCV. IOCV, Riverside.
23. Morisita, M.
1959. Measuring of the dispersion of individuals and analysis of the distributional patterns. Mem. Fac. Sci. Kyushu Univ., Ser. E. Biol. 2: 215-235.
24. Noe, J. P. and C. L. Campbell.
1985. Spatial pattern analysis of plant parasitic nematodes. J. Nematol. 17: 86-93.
25. Permar, T., S. M. Garnsey, D. J. Gumpf, and R. Lee.
1990. A monoclonal antibody that discriminates strains of citrus tristeza virus. Phytopathology 80: 224-228.
26. Upton, G. and B. Fingleton.
1984. Spatial data analysis by example. John Wiley and Sons, Chichester, England. 400 pp.
27. Vanderplank, J. E.
1963. Plant Diseases: Epidemics and Control. Academic Press, New York. 349 pp.
28. Vela, C., M. Cambra, E. Cortes, P. Moreno, J. G. Miguet, C. Perez de San Roman, and A. Sanz.
1986. Production and characterization of monoclonal antibodies specific for citrus tristeza virus and their uses for diagnosis. J. Gen. Virol. 67: 91-96.
29. Vela, C., M. Cambra, A. Sanz, and P. Moreno.
1986. Use of specific monoclonal antibodies for diagnosis of citrus tristeza virus, p. 55-61. *In:* Proc. 10th Conf. IOCV. IOCV, Riverside.